Density functional perturbation theory for lattice dynamics with fully relativistic ultrasoft pseudopotentials: Application to fcc-Pt and fcc-Au

Andrea Dal Corso
Scuola Internazionale Superiore di Studi Avanzati (SISSA) via Beirut 2/4, I-34014 Trieste, Italy and DEMOCRITOS-INFM, I-34014 Trieste, Italy
(Received 26 April 2007; published 24 August 2007)

I present density functional perturbation theory for lattice dynamics with the fully relativistic ultrasoft pseudopotentials (PPs) introduced recently for dealing with spin-orbit effects and use it to calculate the phonon dispersions of fcc-Pt and fcc-Au. The results are compared with the dispersions obtained by scalar relativistic PPs and by inelastic neutron scattering. It is found that, on the phonon spectrum of fcc-Au, spin-orbit effects are small, essentially within the numerical accuracy. In fcc-Pt, these effects, although still small, improve the agreement between theory and experiment close to the Kohn anomaly of the T_1 branch along the Σ line.

DOI: 10.1103/PhysRevB.76.054308 PACS number(s): 63.10.+a, 63.20.Dj, 71.15.Dx, 71.15.Rf

I. INTRODUCTION

More and more often, the theoretical analysis of the experimental inelastic neutron scattering data and of infrared and Raman spectra of molecules, solids, and nanostructures is carried out with the help of vibrational frequencies and displacement eigenvectors calculated within density functional theory (DFT).[1–7] First-principles vibrational free energies are key ingredients for the study of temperature and pressure dependent material properties,[1] and also the superconducting and normal state properties of conventional superconductors are addressed by techniques which rely on accurate phonon dispersions and electron-phonon couplings.[8,9] Density functional perturbation theory[1,10] (DFPT) plays an important role in these applications because it provides the dynamical matrix of a periodic solid at any wave vector with a numerical effort comparable to that required for the ground state.

DFPT is implemented in several free software codes,[11–13] and it can be based either on all-electron methods[14–16] or on plane wave and pseudopotential approaches.[1,17] A few years ago, I presented a generalization of DFPT[18,19] for dealing with ultrasoft pseudopotentials (US-PPs),[20] which has been used to address the vibrational properties of several systems: magnetic and nonmagnetic metals (bcc-Fe,[21] fcc-Ni,[21] Ni_2MnGa,[7] fcc-Cu,[18] fcc-Ag,[18] and fcc-Au[18]), superconducting materials (C_6Ca,[9] and transition metal carbides and nitrides[22]), isolated molecules [nitrobenzene,[19] magnesium phthalocyanine,[23] and C_{60} (Ref. 24)], and atoms and molecules adsorbed on surfaces.[25,26]

So far, in these applications, the US-PPs have been constructed starting from the nonrelativistic or the scalar relativistic[27] (SR) solutions of the atomic problem where spin-orbit effects are neglected. The use of SR-PPs is usually justified by the assumption that spin-orbit coupling has small effects on the phonon vibrational frequencies. This approximation is particularly good for systems made by light elements, but it might be less accurate when dealing with heavy elements whose electronic structure is considerably modified by the spin-orbit coupling. Qualitatively, one can argue that in metals, the phonon dispersions around the Kohn anomalies[28] should have spin-orbit-induced features which cannot be reproduced by SR-PPs. If the topology of the Fermi surface is modified by spin orbit and some Kohn wave vectors change, the Kohn anomalies could move or could have a different shape. Quantitatively, it is instead more difficult to estimate the size of spin-orbit effects on the overall phonon dispersions. Recently, I introduced fully relativistic (FR) US-PPs,[29] which are constructed starting from the large components of the solutions of the atomic radial Dirac-like equation derived in the framework of relativistic DFT.[30] In Ref. 29, the method has been applied to fcc-Pt and fcc-Au. It has been shown that these PPs, which are used within a DFT scheme based on two-component spinor wave functions, yield the same electronic structure as a FR four-component Dirac-like equation.[29] In agreement with previous all-electron calculations, it was found that the lattice constants and the bulk moduli of fcc-Au and fcc-Pt are not significantly modified by the spin-orbit coupling, but the effect on the phonon dispersions was not studied.

In this paper, I generalize DFPT in order to use it together with FR US-PPs, and I present a comparison of the phonon dispersions of fcc-Au and fcc-Pt calculated with the SR and FR US-PPs. I find that, in fcc-Au, spin-orbit coupling has a small effect on the calculated frequencies, essentially within the numerical accuracy. In fcc-Pt, spin-orbit effects remain quite small, but they change the phonon dispersion close to the anomaly of the T_1 branch along the Σ line.[31] Both the SR and FR US-PPs reproduce the anomaly, but its frequency–wave vector dependence is closer to the experimental $T=90$ K data with FR-PPs.

II. THEORY

Within the spin DFT,[32] the total energy of N interacting electrons in an external potential is a functional of the spin density matrix or, equivalently, a functional of the charge $n(\mathbf{r})$ and magnetization $\mathbf{m}(\mathbf{r})$ densities. As in the Kohn-Sham approach,[33] this functional can be written by introducing one-electron two-component spinor wave functions, $\Psi_i^\sigma(\mathbf{r})$, which describe an auxiliary noninteracting electron gas with the same density matrix as the interacting electrons. It is convenient to decompose the total energy into four terms:[19]

$E_{tot}[\Psi_i]=\bar{E}[\Psi_i]+F[n(\mathbf{r}),|\mathbf{m}(\mathbf{r})|]+U_{II}+E_{met}$. U_{II} is the ion-ion interaction energy, while E_{met} is a correction term nonvanishing in metals and in systems with fractional occupation numbers.[19,34] These two terms are the same as in the SR theory[1] and are not discussed further on.

$$F[n(\mathbf{r}),|\mathbf{m}(\mathbf{r})|]=\int d^3r V_{loc}(\mathbf{r})n(\mathbf{r})+E_{Hxc}[n(\mathbf{r}),|\mathbf{m}(\mathbf{r})|] \tag{1}$$

depends on the spinor wave functions implicitly through the charge and the modulus of the magnetization densities.[35] Here, $V_{loc}(\mathbf{r})$ is the local part of the external potential and E_{Hxc} is the Hartree and exchange-correlation energy. $\bar{E}[\Psi_i]$ depends on the spinor wave functions explicitly. When the nuclei and core electrons are described by FR US-PPs,[29] it is given by (in a.u.)

$$\bar{E}[\Psi_i]=-\frac{1}{2}\sum_{i,\sigma}\tilde{\theta}_{F,i}\langle\Psi_i^\sigma|\nabla^2|\Psi_i^\sigma\rangle+\sum_{i,\sigma,\sigma'}\tilde{\theta}_{F,i}\langle\Psi_i^\sigma|V_{NL}^{\sigma,\sigma'}|\Psi_i^{\sigma'}\rangle, \tag{2}$$

where σ and σ' are spin indices. The sum over i runs over all the states, and $\tilde{\theta}_{F,i}$ are the occupation numbers (see Ref. 19). $V_{NL}^{\sigma,\sigma'}$, the nonlocal part of the external potential, is a 2×2 matrix in spin space, nondiagonal for FR-PPs, and a multiple of the 2×2 identity matrix for SR-PPs. As discussed in detail in Ref. 29, for FR US-PPs, $V_{NL}^{\sigma,\sigma'}$ is given by

$$V_{NL}^{\sigma,\sigma'}(\mathbf{r}_1,\mathbf{r}_2)=\sum_{I,n,m}D_{n,m}^{\gamma(I),\sigma,\sigma'}\beta_n^{\gamma(I)}(\mathbf{r}_1-\mathbf{R}_I)\beta_m^{*\gamma(I)}(\mathbf{r}_2-\mathbf{R}_I), \tag{3}$$

where $D_{n,m}^{\gamma(I),\sigma,\sigma'}$ are spin-dependent PP coefficients and $\beta_n^{\gamma(I)}\times(\mathbf{r}-\mathbf{R}_I)=\beta_{\tau,l,j}^{\gamma(I)}(|\mathbf{r}-\mathbf{R}_I|)Y_{l,m_l}(\Omega_{\mathbf{r}-\mathbf{R}_I})$ are projector functions factorized into radial functions and spherical harmonics. I runs over all the atoms, $\mathbf{R}_I$ are the atomic positions, and $\gamma(I)$ identify the atomic types. The index n (as well as m) is a shorthand notation for the four indices τ,l,j,m_l (see Ref. 29).

The density matrix is a quadratic functional of the orbitals:

$$n^{\sigma,\sigma'}(\mathbf{r})=\sum_{i,\sigma_1,\sigma_2}\tilde{\theta}_{F,i}\langle\Psi_i^{\sigma_1}|K_{\sigma_1,\sigma_2}^{\sigma,\sigma'}(\mathbf{r})|\Psi_i^{\sigma_2}\rangle, \tag{4}$$

and the electron density is the trace of the density matrix, $n(\mathbf{r})=\Sigma_\sigma n^{\sigma,\sigma}(\mathbf{r})$, while the magnetization density is given by the product of the density matrix and the Pauli matrices $\boldsymbol{\sigma}$: $\mathbf{m}(\mathbf{r})=\mu_B\Sigma_{\sigma,\sigma'}n^{\sigma,\sigma'}(\mathbf{r})\boldsymbol{\sigma}^{\sigma,\sigma'}$ (μ_B is the Bohr magneton). In the present formalism, the operator $K_{\sigma_1,\sigma_2}^{\sigma,\sigma'}(\mathbf{r})$, defined through the augmentation functions $Q_{n,m}^{\gamma(I)}(\mathbf{r}-\mathbf{R}_I)$ and the projector functions $\beta_n^{\gamma(I)}(\mathbf{r}-\mathbf{R}_I)$ as in the SR case,[29,36] becomes spin dependent through the factors $f_{l,j,m_l;l,j,m_l'}^{\sigma,\sigma'}$ introduced in Ref. 29 to write the spin-angle functions with spherical harmonics:

$$K_{\sigma_1,\sigma_2}^{\sigma,\sigma'}(\mathbf{r};\mathbf{r}_1,\mathbf{r}_2)=\delta(\mathbf{r}-\mathbf{r}_1)\delta(\mathbf{r}-\mathbf{r}_2)\delta_{\sigma,\sigma_1}\delta_{\sigma',\sigma_2}+\sum_{I,n,m}\sum_{n_1,m_1}Q_{n,m}^{\gamma(I)}(\mathbf{r}-\mathbf{R}_I)\times f_{n_1,n}^{\sigma_1,\sigma}\beta_{n_1}^{\gamma(I)}(\mathbf{r}_1-\mathbf{R}_I)f_{m,m_1}^{\sigma',\sigma_2}\beta_{m_1}^{*\gamma(I)}(\mathbf{r}_2-\mathbf{R}_I), \tag{5}$$

where the symbol $f_{n,m}^{\sigma,\sigma'}$ stands for $f_{n,m}^{\sigma,\sigma'}=f_{\tau,l,j,m_l;\tau',l',j',m_l'}^{\sigma,\sigma'}=f_{l,j,m_l;l,j,m_l'}^{\sigma,\sigma'}\delta_{\tau,\tau'}\delta_{l,l'}\delta_{j,j'}$. For the integral of the charge density to be equal to the total number of electrons, the orbitals $|\Psi_i^\sigma\rangle$ must obey generalized orthonormalization constraints $\Sigma_{\sigma,\sigma'}\langle\Psi_i^\sigma|S^{\sigma,\sigma'}|\Psi_j^{\sigma'}\rangle=\delta_{i,j}$, where $S^{\sigma,\sigma'}(\mathbf{r}_1,\mathbf{r}_2)=\Sigma_{\sigma_1}\int d^3rK_{\sigma,\sigma'}^{\sigma_1,\sigma_1}(\mathbf{r};\mathbf{r}_1,\mathbf{r}_2)$ is the overlap matrix (see also Ref. 29).

Written in this compact form, the total energy functional is formally similar to the functional used in Ref. 19 to derive DFPT with SR US-PPs. The dynamical matrix of a solid at any wave vector $\mathbf{q}$ can be determined in the same way, with the additional bookkeeping of the spin indices. Nonetheless, the present functional allows the description of magnetic as well as nonmagnetic systems [for $\mathbf{m}(\mathbf{r})=0$] in the presence of spin-orbit coupling. Moreover, in some limits, one obtains other functionals useful in specific applications. For $f_{n,m}^{\sigma,\sigma'}=\delta_{n,m}\delta_{\sigma,\sigma'}$ and neglecting the total angular momentum index j in n and m, we get the functional which describes unconstrained noncollinear magnetic structures with SR-PPs.[37–40] FR norm-conserving PPs, as those proposed in Ref. 41, lead to the present functional with $Q_{n,m}^{\gamma(I)}(\mathbf{r}-\mathbf{R}_I)=0$, and hence $S^{\sigma,\sigma'}(\mathbf{r}_1,\mathbf{r}_2)=\delta(\mathbf{r}_1-\mathbf{r}_2)\delta_{\sigma,\sigma'}$. The formulas deduced in Ref. 19, valid for SR US-PPs within the local spin density approximation, can be found by setting $f_{n,m}^{\sigma,\sigma'}=\delta_{n,m}\delta_{\sigma,\sigma'}$, taking the magnetization density $\mathbf{m}(\mathbf{r})$ everywhere parallel to a fixed direction and separating the spinor wave functions into spin up or spin down.

By minimizing the total energy functional, we obtain the generalized Kohn-Sham equations for the spinor wave functions:

$$\sum_{\sigma'}H^{\sigma,\sigma'}|\Psi_i^{\sigma'}\rangle=\varepsilon_i\sum_{\sigma'}S^{\sigma,\sigma'}|\Psi_i^{\sigma'}\rangle, \tag{6}$$

with $H^{\sigma,\sigma'}=-\frac{1}{2}\nabla^2\delta_{\sigma,\sigma'}+V_{KS}^{\sigma,\sigma'}$ and $V_{KS}^{\sigma,\sigma'}=V_{NL}^{\sigma,\sigma'}+\Sigma_{\sigma_1,\sigma_2}\int d^3r\, V_{LOC}^{\sigma_1,\sigma_2}(\mathbf{r})K_{\sigma,\sigma'}^{\sigma_1,\sigma_2}(\mathbf{r})$. Here, $V_{LOC}^{\sigma,\sigma'}(\mathbf{r})=V_{eff}(\mathbf{r})\delta_{\sigma,\sigma'}-\mu_B\mathbf{B}_{xc}(\mathbf{r})\cdot\boldsymbol{\sigma}^{\sigma,\sigma'}$ is a spin-dependent local potential defined in terms of the effective potential $V_{eff}=\frac{\delta F}{\delta n}$ and of the exchange-correlation magnetic field $\mathbf{B}_{xc}^\alpha=-\frac{\delta E_{xc}}{\delta\mathbf{m}_\alpha}$. $V_{eff}(\mathbf{r})=V_{loc}(\mathbf{r})+V_{Hxc}(\mathbf{r})$ is the sum of the local and of the Hartree and exchange-correlation potentials, while $\mathbf{B}_{xc}$ is the functional derivative of E_{xc} with respect to the magnetization (see Refs. 19 and 29). For the following, it is useful to define a spin-dependent Hartree and exchange-correlation potential as $V_{Hxc}^{\sigma,\sigma'}(\mathbf{r})=V_{Hxc}(\mathbf{r})\delta_{\sigma,\sigma'}-\mu_B\mathbf{B}_{xc}(\mathbf{r})\cdot\boldsymbol{\sigma}^{\sigma,\sigma'}$, so that $V_{LOC}^{\sigma,\sigma'}(\mathbf{r})=V_{loc}(\mathbf{r})\delta_{\sigma,\sigma'}+V_{Hxc}^{\sigma,\sigma'}(\mathbf{r})$.

The forces acting on the ions, equal to the negative first-order derivative of the total energy with respect to the ionic displacements, can be calculated by the Hellmann-Feynman theorem. Calling λ the amplitude of the displacement $\mathbf{u}_{I,\alpha}$ of the atom I in the direction α, we can write the first-order derivative of the total energy with respect to λ as[42]

$$\frac{dE_{tot}}{d\lambda} = \sum_{i,\sigma} \tilde{\theta}_{F,i} \langle \Psi_i^\sigma | \phi_{\lambda,i}^\sigma \rangle, \tag{7}$$

with

$$|\phi_{\lambda,i}^\sigma\rangle = \sum_{\sigma'} \left[\frac{\partial V_{KS}^{\sigma,\sigma'}}{\partial \lambda} - \varepsilon_i \frac{\partial S^{\sigma,\sigma'}}{\partial \lambda} \right] |\Psi_i^{\sigma'}\rangle, \tag{8}$$

where the partial derivative of $V_{KS}^{\sigma,\sigma'}$ is calculated at fixed orbitals and it is given by

$$\frac{\partial V_{KS}^{\sigma,\sigma'}}{\partial \lambda} = \frac{\partial V_{NL}^{\sigma,\sigma'}}{\partial \lambda} + \sum_{\sigma_1} \int d^3r \frac{\partial V_{loc}(\mathbf{r})}{\partial \lambda} K_{\sigma,\sigma'}^{\sigma_1,\sigma_1}(\mathbf{r}) + \sum_{\sigma_1,\sigma_2} \int d^3r V_{LOC}^{\sigma_1,\sigma_2}(\mathbf{r}) \frac{\partial K_{\sigma,\sigma'}^{\sigma_1,\sigma_2}(\mathbf{r})}{\partial \lambda}. \tag{9}$$

Note that the factors $f_{n,m}^{\sigma,\sigma'}$, which make $K_{\sigma_1,\sigma_2}^{\sigma,\sigma'}(\mathbf{r})$ spin dependent, do not introduce new terms in Eq. (9) because they are products of unitary matrix elements and of Clebsch-Gordan coefficients,[29] which are independent of the atomic positions.

The dynamical matrix at an arbitrary $\mathbf{q}$ point of the Brillouin zone (BZ) is the Fourier transform of the interatomic force constants $\Phi_{I,\alpha;I',\beta}$. Within the Born-Oppenheimer adiabatic approximation, we identify $\Phi_{I,\alpha;I',\beta}$ with the mixed second derivatives of the total energy with respect to the displacements $\mathbf{u}_{I,\alpha}$ and $\mathbf{u}_{I',\beta}$ of the atoms I and I' in the directions α and β, respectively. These derivatives depend on the first-order change of the spinor wave functions. In order to calculate them, we start from the first-order derivative of the density matrix with respect to the displacement $\mathbf{u}_{I',\beta}$, called μ for short, which is given by

$$\frac{dn^{\sigma,\sigma'}(\mathbf{r})}{d\mu} = 2\,\mathrm{Re} \sum_{i,\sigma_1,\sigma_2} \langle \Psi_i^{\sigma_1} | K_{\sigma_1,\sigma_2}^{\sigma,\sigma'}(\mathbf{r}) | \Delta^\mu \Psi_i^{\sigma_2} \rangle - \sum_{i,\sigma_1,\sigma_2} \langle \Psi_i^{\sigma_1} | K_{\sigma_1,\sigma_2}^{\sigma,\sigma'}(\mathbf{r}) | \delta^\mu \Psi_i^{\sigma_2} \rangle + \sum_{i,\sigma_1,\sigma_2} \tilde{\theta}_{F,i} \left\langle \Psi_i^{\sigma_1} \left| \frac{\partial K_{\sigma_1,\sigma_2}^{\sigma,\sigma'}(\mathbf{r})}{\partial \mu} \right| \Psi_i^{\sigma_2} \right\rangle, \tag{10}$$

where, as in Ref. 19, we have introduced two auxiliary spinor wave functions:

$$|\Delta^\mu \Psi_i^\sigma\rangle = \frac{1}{2\eta} \tilde{\delta}_{F,i} \frac{d\varepsilon_F}{d\mu} |\Psi_i^\sigma\rangle + \sum_{j,\sigma_1,\sigma_2} \frac{\tilde{\theta}_{F,i} - \tilde{\theta}_{F,j}}{\varepsilon_i - \varepsilon_j} \theta_{j,i} |\Psi_j^\sigma\rangle \langle \Psi_j^{\sigma_1}| \times \left[\frac{dV_{KS}^{\sigma_1,\sigma_2}}{d\mu} - \varepsilon_i \frac{\partial S^{\sigma_1,\sigma_2}}{\partial \mu} \right] |\Psi_i^{\sigma_2}\rangle \tag{11}$$

and

$$|\delta^\mu \Psi_i^\sigma\rangle = \sum_{j,\sigma_1,\sigma_2} [\tilde{\theta}_{F,i}\theta_{i,j} + \tilde{\theta}_{F,j}\theta_{j,i}] |\Psi_j^\sigma\rangle \left\langle \Psi_j^{\sigma_1} \left| \frac{\partial S^{\sigma_1,\sigma_2}}{\partial \mu} \right| \Psi_i^{\sigma_2} \right\rangle. \tag{12}$$

The first term in Eq. (11), due to the change of the Fermi energy induced by an atomic displacement, is illustrated in Ref. 19. To calculate the other term that would involve a sum over all the conduction states, we can introduce a linear system whose solutions are the spinor wavefunctions: $|\tilde{\Delta}^\mu \Psi_i^\sigma\rangle = |\Delta^\mu \Psi_i^\sigma\rangle - \frac{1}{2\eta} \tilde{\delta}_{F,i} \frac{d\varepsilon_F}{d\mu} |\Psi_i^\sigma\rangle$. Following Ref. 34, we write

$$\sum_{\sigma'} \left[-\frac{1}{2}\nabla^2 \delta_{\sigma,\sigma'} + V_{KS}^{\sigma,\sigma'} + Q^{\sigma,\sigma'} - \varepsilon_i S^{\sigma,\sigma'} \right] |\tilde{\Delta}^\mu \Psi_i^{\sigma'}\rangle = -\sum_{\sigma'\sigma''} P_{c,i}^{\dagger,\sigma,\sigma'} \left[\frac{dV_{KS}^{\sigma',\sigma''}}{d\mu} - \varepsilon_i \frac{\partial S^{\sigma',\sigma''}}{\partial \mu} \right] |\Psi_i^{\sigma''}\rangle, \tag{13}$$

with

$$P_{c,i}^{\dagger\sigma,\sigma'} = \left[\tilde{\theta}_{F,i} \delta_{\sigma,\sigma'} - \sum_{j,\sigma_1} \beta_{i,j} S^{\sigma,\sigma_1} |\Psi_j^{\sigma_1}\rangle \langle \Psi_j^{\sigma'}| \right]. \tag{14}$$

$\beta_{i,j}$ are calculated as in Refs. 19 and 34. $Q^{\sigma,\sigma'}$ is an operator, vanishing on the conduction states, which makes the linear system nonsingular: $Q^{\sigma,\sigma'} = \Sigma_{j,\sigma_1,\sigma_2} \alpha_j S^{\sigma,\sigma_1} |\Psi_j^{\sigma_1}\rangle \langle \Psi_j^{\sigma_2}| S^{\sigma_2,\sigma'}$, where the α_j are discussed in Refs. 19 and 34. In Eq. (13), the right-hand side depends on the variation of the spin-dependent Hartree and exchange-correlation potential:

$$\sum_{\sigma'} \left[\frac{dV_{KS}^{\sigma,\sigma'}}{d\mu} - \varepsilon_i \frac{\partial S^{\sigma,\sigma'}}{\partial \mu} \right] |\Psi_i^{\sigma'}\rangle = |\phi_{\mu,i}^\sigma\rangle + \sum_{\sigma_1,\sigma_2,\sigma'} \int d^3r \frac{dV_{Hxc}^{\sigma_1,\sigma_2}(\mathbf{r})}{d\mu} K_{\sigma,\sigma'}^{\sigma_1,\sigma_2}(\mathbf{r}) |\Psi_i^{\sigma'}\rangle. \tag{15}$$

The latter depends linearly on the variation of the charge and magnetization densities:

$$\frac{dV_{Hxc}^{\sigma,\sigma'}(\mathbf{r})}{d\mu} = \left[\frac{\delta V_{Hxc}}{\delta n} \frac{dn(\mathbf{r})}{d\mu} + \sum_{\alpha=1}^{3} \frac{\delta V_{Hxc}}{\delta \mathbf{m}_\alpha} \frac{d\mathbf{m}_\alpha(\mathbf{r})}{d\mu} \right] \delta_{\sigma,\sigma'} - \mu_B \sum_{\beta=1}^{3} \left[\frac{\delta \mathbf{B}_{xc}^\beta}{\delta n} \frac{dn(\mathbf{r})}{d\mu} + \sum_{\alpha=1}^{3} \frac{\delta \mathbf{B}_{xc}^\beta}{\delta \mathbf{m}_\alpha} \frac{d\mathbf{m}_\alpha(\mathbf{r})}{d\mu} \right] \boldsymbol{\sigma}_\beta^{\sigma,\sigma'}, \tag{16}$$

and hence, it depends linearly on the first-order derivative of the density matrix $\frac{dn^{\sigma,\sigma'}(\mathbf{r})}{d\mu}$. Therefore, Eqs. (10), (13), (15), and (16) form a set of self-consistent equations which can be solved with the same techniques used for the SR US-PPs.

Once the change of the wave functions $|\Delta^{\mu}\Psi_i^{\sigma}\rangle$ has been calculated, one can obtain the mixed second-order derivatives of the total energy with respect to two atomic displacements. As in Ref. 19, the differentiation of the Hellmann-Feynman forces [Eq. (7)] with respect to μ gives four terms. The first term, depending on the unperturbed wave functions, is

$$\frac{d^2E_{tot}^{(1)}}{d\mu d\lambda} = \sum_{i,\sigma,\sigma'} \tilde{\theta}_{F,i} \langle \Psi_i^{\sigma} | \left[\frac{\partial^2 V_{KS}^{\sigma,\sigma'}}{\partial\mu\partial\lambda} - \varepsilon_i \frac{\partial^2 S^{\sigma,\sigma'}}{\partial\mu\partial\lambda} \right] | \Psi_i^{\sigma'} \rangle, \tag{17}$$

where $\frac{\partial^2 V_{KS}^{\sigma,\sigma'}}{\partial\mu\partial\lambda}$ is calculated at fixed orbitals:

$$\frac{\partial^2 V_{KS}^{\sigma,\sigma'}}{\partial\mu\partial\lambda} = \frac{\partial^2 V_{NL}^{\sigma,\sigma'}}{\partial\mu\partial\lambda} + \sum_{\sigma_1} \int d^3r \frac{\partial^2 V_{loc}(\mathbf{r})}{\partial\mu\partial\lambda} K_{\sigma,\sigma'}^{\sigma_1,\sigma_1}(\mathbf{r}) + \sum_{\sigma_1,\sigma_2} \int d^3r V_{LOC}^{\sigma_1,\sigma_2}(\mathbf{r}) \frac{\partial^2 K_{\sigma,\sigma'}^{\sigma_1,\sigma_2}(\mathbf{r})}{\partial\mu\partial\lambda} + \left[\sum_{\sigma_1} \int d^3r \frac{\partial V_{loc}(\mathbf{r})}{\partial\lambda} \frac{\partial K_{\sigma,\sigma'}^{\sigma_1,\sigma_1}(\mathbf{r})}{\partial\mu} + (\lambda \leftrightarrow \mu) \right]. \tag{18}$$

The second term, depending on the solution of the linear system [Eq. (13)], is

$$\frac{d^2E_{tot}^{(2)}}{d\mu d\lambda} = 2\,\mathrm{Re} \sum_{i,\sigma} \langle \Delta^{\mu}\Psi_i^{\sigma} | \phi_{\lambda,i}^{\sigma} \rangle. \tag{19}$$

For norm-conserving PPs, these two terms give the complete expression of the mixed second-order derivative of the total energy, while in the US-PP scheme, one must consider two additional contributions which have no correspondent counterparts in the norm-conserving scheme.[18,19] As in the SR case, the third term is the integral of the product of the change of the augmentation density matrix $\Delta^{\mu}n^{\sigma,\sigma'}(\mathbf{r})$, equal to the last two terms in Eq. (10), and the change of the spin-dependent Hartree and exchange-correlation potential:

$$\frac{d^2E_{tot}^{(3)}}{d\mu d\lambda} = \sum_{\sigma,\sigma'} \int d^3r \frac{\partial V_{Hxc}^{\sigma,\sigma'}(\mathbf{r})}{\partial\lambda} \Delta^{\mu}n^{\sigma,\sigma'}(\mathbf{r}), \tag{20}$$

while the fourth term, due to dependence of the orthogonality constraint on the atomic positions, is given by

$$\frac{d^2E_{tot}^{(4)}}{d\mu d\lambda} = -\sum_{i,\sigma} [\langle \delta^{\mu}\Psi_i^{\sigma} | \phi_{\lambda,i}^{\sigma} \rangle + (\mu \leftrightarrow \lambda)]. \tag{21}$$

As shown in Ref. 19, by using these expressions, it is straightforward to derive the dynamical matrix at any wave vector **q**. Due to the formal analogy between Eqs. (18)–(21) and Eqs. (39), (40), (41), and (42) of Ref. 19, the result is not essentially different and is not repeated here. The final expressions are implemented in the QUANTUM-ESPRESSO package,[11] and the code is publicly available.

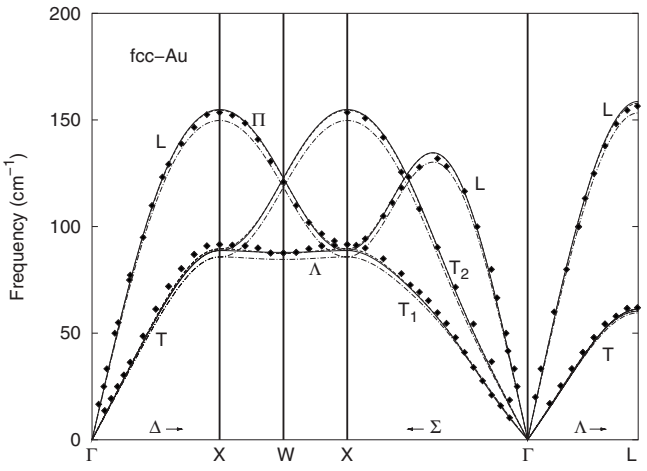

FIG. 1. Calculated LDA phonon dispersions at $T=0$ K for fcc-Au obtained with FR US-PPs (solid lines), compared with dispersions obtained with SR US-PPs (dashed lines) and inelastic neutron scattering data at $T=295$ K from Ref. 47 (solid diamonds). Dot dashed lines are obtained with FR-PPs at $a_0=7.67$ a.u., the estimated theoretical lattice constant at $T=295$ K.

III. APPLICATIONS

In this section, the above theory is used to calculate the phonon dispersions of fcc-Au and of fcc-Pt. DFT calculations are carried out within the local density approximation (LDA) with the Perdew and Zunger[43] parametrization of the exchange and correlation energy. The PPs of Au and Pt are described in Ref. 29.[44] The kinetic energy cutoffs are 30 and 250 Ry for the pseudo-wave-functions and for the charge density, respectively. Monkhorst-Pack special **k**-point grids[45] of $12\times12\times12$ and $24\times24\times24$ points are used for the integration over the BZ of fcc-Au and fcc-Pt, respectively. The smearing approach of Ref. 46 is used for dealing with the Fermi surface. The smearing parameter is $\eta=0.01$ Ry in fcc-Au, while it is $\eta=0.005$ Ry in fcc-Pt, due to the presence of a Kohn anomaly in the T_1 branch along the Σ line (see below).[31] In fcc-Au (fcc-Pt), the dynamical matrices are calculated in a $4\times4\times4$ ($8\times8\times8$) **q**-point grid and a Fourier interpolation is used to obtain phonon frequencies in the other points of the BZ. The phonon dispersions are calculated at the theoretical lattice constants, which turn out to be $a_0=7.65$ a.u. (7.64 a.u.) with the SR (FR)-PPs in fcc-Au, and $a_0=7.41$ a.u. (7.40 a.u.) in fcc-Pt.

The phonon dispersions of fcc-Au calculated with SR (dashed lines) and with FR (solid lines) PPs are shown in Fig. 1. Conventional names of the phonon dispersion branches are taken from Ref. 31. Diamonds indicate the experimental inelastic neutron scattering data measured at room temperature (295 K).[47] On the scale of the figure, the FR phonon dispersions are barely distinguishable from the SR ones. The calculated frequencies at the main symmetry points of the BZ are reported in Table I. In these points, the largest difference between SR and FR results is about 2 cm^{-1} at L, comparable with the numerical accuracy of the calculation. This result is not surprising because in Au the $5d$ shell is completely filled and the spin-orbit coupling does not

TABLE I. LDA frequencies calculated at selected points of the BZ for the two metals studied in this work. All frequencies are in cm^{-1}. Experimental data are at $T=295$ K from Ref. 47 for fcc-Au, and at $T=90$ K from Ref. 31 for fcc-Pt.

	a_0 (a.u.)	X_T	X_L	W_Λ	W_Π	L_T	L_L
				fcc-Au			
SR	7.65 (7.68)	89(86)	154(149)	87(83)	122(118)	60(58)	158(152)
FR	7.64 (7.67)	89(86)	155(150)	88(84)	123(118)	62(59)	159(153)
Expt.	7.67[a]	92	154	88	121	62	157
				fcc-Pt			
SR	7.41	131	196	115	159	95	201
FR	7.40	130	195	118	159	97	200
Expt.	7.40[b]	128	193	108	155	97	195

[a]Extrapolated at $T=0$ K values.
[b]Reference 51.

change the Fermi surface, which is determined by bands with mainly 6*s* character.

In order to compare theoretical and experimental results, we have to keep into account that the uncertainty of the measured values, though not uniform in all the BZ, is of the order of a few cm^{-1}.[47] Furthermore, our results are obtained at the $T=0$ K theoretical lattice constant, while the experimental data are measured at 295 K and are influenced by anharmonic effects. The order of magnitude of the anharmonic effects can be estimated by comparing the phonon frequencies calculated at the $T=0$ K and at the $T=295$ K lattice constants. From the experimental thermal expansion coefficient, the lattice constant at $T=295$ K can be estimated to be about 0.4% larger than that at $T=0$ K. It is therefore $a_0=7.68$ a.u. and $a_0=7.67$ a.u. in the SR and FR cases, respectively. As can be seen from the calculated values reported in Table I and from the FR dispersions reported in Fig. 1, the lattice expansion actually softens by about 3%–4% of the theoretical frequencies that become slightly lower than experiment. A recent calculation performed at $a_0=7.71$ a.u., the experimental room temperature lattice constant, is in agreement with this conclusion.[48] In fcc-Cu and fcc-Ag, the LDA approximation overestimates the phonon frequencies,[18] and in fcc-Cu, the generalized gradient approximation is known to underestimate them.[49] In this respect, Au differs from the other two noble metals having LDA frequencies lower than experiment. This is found both with SR- and with FR-PPs.

The phonon dispersions of fcc-Pt calculated with SR (dashed lines) and with FR (solid lines) PPs are shown in Fig. 2. Diamonds indicate the experimental inelastic neutron scattering data measured at 90 K.[31] The theoretical and experimental frequencies at the main symmetry points of the BZ are reported in Table I. The differences between FR and SR results are of the order of 1–2 cm^{-1}, so on the overall phonon spectrum the spin-orbit effects are quite small. The agreement with experiment is very good in both cases, with errors almost always lower than 5 cm^{-1}. There is an exception at the *W* point, where the SR result has an error of 7 cm^{-1}, while the FR result is 10 cm^{-1} higher than the experimental value (that in this point has an estimated uncertainty of 2.7 cm^{-1}). In the case of fcc-Pt, the anharmonic effects on the experimental data should be quite small. Actually, the thermal expansion is smaller than that of fcc-Au and the experiment is done at $T=90$ K. The lattice constant at this temperature differs from that at $T=0$ K by less than 0.1%.

In Fig. 2, we can observe a sizable difference between SR and FR results on the T_1 branch along the Σ direction. Experimentally, it is known that Pt has an anomaly in the T_1 branch, which has been suggested to be a Kohn anomaly.[31] A Kohn anomaly is a jump in the first derivative of the frequency–wave vector curve due to a sudden change of the screening properties of the electron gas at particular wave vectors. It is visible in the phonon dispersion curve as a sudden change of the slope.[28] In platinum, the anomaly of the T_1 branch has been explained by the presence of Kohn wave vectors parallel to the Σ direction, which join different points in the heavy hole cylinder in the experimental Fermi

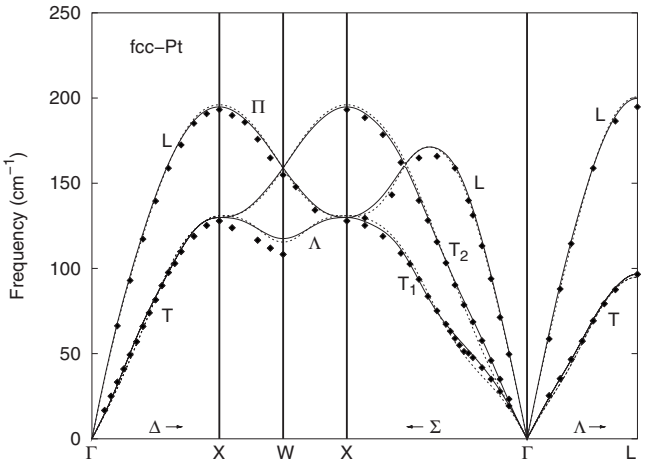

FIG. 2. Calculated LDA phonon dispersions at $T=0$ K for fcc-Pt obtained with FR US-PPs (solid lines), compared with dispersions obtained with SR US-PPs (dashed lines) and inelastic neutron scattering data at $T=90$ K from Ref. 31 (solid diamonds).

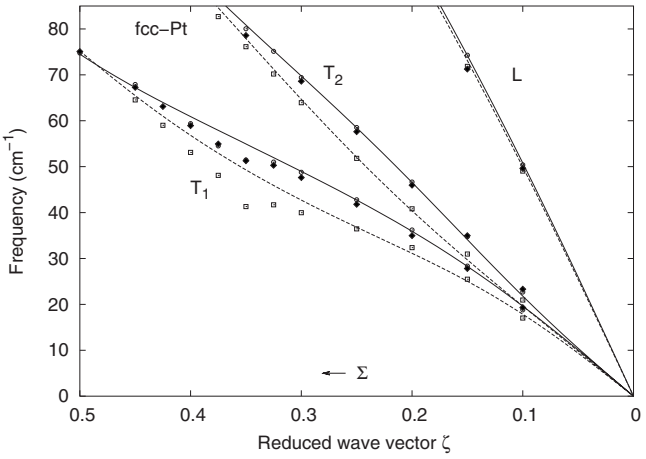

FIG. 3. Calculated LDA phonon dispersions for fcc-Pt in the Σ direction [$\mathbf{k}=(\zeta,\zeta,0)$ in units $2\pi/a_0$]. Solid (dashed) lines show results obtained with FR (SR) US-PPs by interpolating on the $8\times8\times8$ **q**-point grid. Empty circles (squares) are the results of a DFPT evaluation of the phonon frequencies with FR (SR) PPs, while inelastic neutron scattering data from Ref. 31 are shown by solid diamonds.

surface.[31] A similar anomaly in Pd has been addressed recently by using *ab initio* techniques.[50] The anomaly leads to long range interatomic force constants and therefore, in this part of the spectrum, it is difficult to compare SR and FR results using the Fourier interpolation, which could introduce a significant error. Actually, with the $8\times8\times8$ **q**-point grid, close to the anomaly, only the two points $\mathbf{q}=(0.25,0.25,0.0)$ and $\mathbf{q}=(0.5,0.5,0.0)$ (in units of $2\pi/a_0$) are calculated by DFPT. Therefore, the phonon frequencies in several points along the Σ direction have been recalculated directly via DFPT and the results are shown in Fig. 3, in an enlarged scale. In agreement with the fact that the Kohn wave vectors that join the heavy hole cylinder are not substantially changed by the spin-orbit coupling, both the SR and the FR dispersions present the anomaly at about $\mathbf{q}=(0.35,0.35,0.0)$. However, the SR-PP gives a much stronger anomaly with lower frequencies with respect to the FR-PP. The FR results turn out to follow the experimental data taken at $T=90$ K. It has to be noted that the shape of the anomaly is temperature dependent. While less pronounced, it is still visible at room temperature and also at $T=473$ K.[31]

From Fig. 3 we can also see that, close to the Γ point, along the Σ direction, the frequencies of the T_2 phonon branch calculated with SR-PP are too low with respect to experiment, which is instead reproduced by the FR-PP.

ACKNOWLEDGMENTS

The work was sponsored by MIUR PRIN/Cofin Contract No. 2004023199, as well as by INFM/CNR "Iniziativa transversale calcolo parallelo." Part of the calculations have been done on the SP5 at CINECA in Bologna.

[1] S. Baroni, S. de Gironcoli, A. Dal Corso, and P. Giannozzi, Rev. Mod. Phys. **73**, 515 (2001).
[2] P. Umari, X. Gonze, and A. Pasquarello, Phys. Rev. Lett. **90**, 027401 (2003).
[3] L. Wirtz, M. Lazzeri, F. Mauri, and A. Rubio, Phys. Rev. B **71**, 241402(R) (2005).
[4] N. Mounet and N. Marzari, Phys. Rev. B **71**, 205214 (2005).
[5] F. Giustino, Jonathan R. Yates, I. Souza, M. L. Cohen, and S. G. Louie, Phys. Rev. Lett. **98**, 047005 (2007).
[6] R. Lazzari, N. Vast, J. M. Besson, S. Baroni, and A. Dal Corso, Phys. Rev. Lett. **83**, 3230 (1999).
[7] C. Bungaro, K. M. Rabe, and A. Dal Corso, Phys. Rev. B **68**, 134104 (2003).
[8] G. Profeta, C. Franchini, N. N. Lathiotakis, A. Floris, A. Sanna, M. A. L. Marques, M. Lüders, S. Massidda, E. K. U. Gross, and A. Continenza, Phys. Rev. Lett. **96**, 047003 (2006).
[9] M. Calandra and F. Mauri, Phys. Rev. Lett. **95**, 237002 (2005).
[10] S. Baroni, P. Giannozzi, and A. Testa, Phys. Rev. Lett. **58**, 1861 (1987).
[11] See http://www.quantum-espresso.org
[12] See http://www.abinit.org
[13] See http://www.physics.ucdavis.edu/~mindlab/
[14] R. Yu and H. Krakauer, Phys. Rev. B **49**, 4467 (1994).
[15] S. Y. Savrasov and D. Y. Savrasov, Phys. Rev. B **54**, 16487 (1996).
[16] R. Heid and K.-P. Bohnen, Phys. Rev. B **60**, R3709 (1999).
[17] X. Gonze and C. Lee, Phys. Rev. B **55**, 10355 (1997).
[18] A. Dal Corso, A. Pasquarello, and A. Baldereschi, Phys. Rev. B **56**, R11369 (1997).
[19] A. Dal Corso, Phys. Rev. B **64**, 235118 (2001).
[20] D. Vanderbilt, Phys. Rev. B **41**, 7892 (1990).
[21] A. Dal Corso and S. de Gironcoli, Phys. Rev. B **62**, 273 (2000).
[22] E. I. Isaev, R. Ahuja, S. I. Simak, A. I. Lichtenstein, Yu. Kh. Vekilov, B. Johansson, and I. A. Abrikosov, Phys. Rev. B **72**, 064515 (2005).
[23] J. Tóbik and E. Tosatti, Surf. Sci. **600**, 3995 (2006).
[24] N. Manini, A. Dal Corso, M. Fabrizio, and E. Tosatti, Philos. Mag. B **73**, 793 (2001).
[25] N. Bonini, A. Kokalj, A. Dal Corso, S. de Gironcoli, and S. Baroni, Phys. Rev. B **69**, 195401 (2004).
[26] N. Bonini, A. Kokalj, A. Dal Corso, S. de Gironcoli, and S. Baroni, Surf. Sci. **600**, 5074 (2006).
[27] D. D. Koelling and B. N. Harmon, J. Phys. C **10**, 3107 (1977).
[28] W. Kohn, Phys. Rev. Lett. **2**, 393 (1959).
[29] A. Dal Corso and A. M. Conte, Phys. Rev. B **71**, 115106 (2005).
[30] A. H. MacDonald and S. H. Vosko, J. Phys. C **12**, 2977 (1979); A. K. Rajagopal and J. Callaway, Phys. Rev. B **7**, 1912 (1973).
[31] D. H. Dutton, B. N. Brockhouse, and A. P. Miiller, Can. J. Phys. **50**, 2915 (1972).
[32] L. Hedin and B. I. Lundqvist, J. Phys. C **4**, 2064 (1971).
[33] W. Kohn and L. J. Sham, Phys. Rev. **140**, A1133 (1965).
[34] S. de Gironcoli, Phys. Rev. B **51**, 6773 (1995).
[35] In this paper, we do not consider the dependence of the exchange-correlation energy on the gradient of the charge and of the mag-

netization densities, which is a question that will be addressed in the future.

[36] A. Pasquarello, K. Laasonen, R. Car, C. Lee, and D. Vanderbilt, Phys. Rev. Lett. **69**, 1982 (1992); K. Laasonen, A. Pasquarello, R. Car, C. Lee, and D. Vanderbilt, Phys. Rev. B **47**, 10142 (1993).

[37] R. Gebauer and S. Baroni, Phys. Rev. B **61**, R6459 (2000).

[38] T. Oda, A. Pasquarello, and R. Car, Phys. Rev. Lett. **80**, 3622 (1998).

[39] D. Hobbs, G. Kresse, and J. Hafner, Phys. Rev. B **62**, 11556 (2000).

[40] Ph. Kurz, F. Förster, L. Nordström, G. Bihlmayer, and S. Blügel, Phys. Rev. B **69**, 024415 (2004).

[41] G. Theurich and N. A. Hill, Phys. Rev. B **64**, 073106 (2001).

[42] In this formula, the terms due to the nonlinear core correction approximation (NLCC) of S. G. Louie, S. Froyen, and M. L. Cohen, Phys. Rev. B **26**, 1738 (1982) are not written. These terms are treated in detail in Ref. 19 and are not changed by the present scheme. The NLCC approximation is used in the Pt calculations.

[43] J. P. Perdew and A. Zunger, Phys. Rev. B **23**, 5048 (1981).

[44] In the present work, the SR-PP of Pt has been generated with the electronic configuration $5d^9 6s^1 6p^0$. The core radius for the $6p$ channel was 2.6 a.u. The other parameters, as well as the other PPs, are as in Ref. 29. At the high symmetry points, this PP has phonon frequencies $3-4$ cm^{-1} lower than the PP used in Ref. 29.

[45] H. J. Monkhorst and J. D. Pack, Phys. Rev. B **13**, 5188 (1976).

[46] M. Methfessel and A. T. Paxton, Phys. Rev. B **40**, 3616 (1989).

[47] J. W. Lynn, H. G. Smith, and R. M. Nicklow, Phys. Rev. B **8**, 3493 (1973).

[48] P. Souvatzis, A. Delin, and O. Eriksson, Phys. Rev. B **73**, 054110 (2006).

[49] F. Favot and A. Dal Corso, Phys. Rev. B **60**, 11427 (1999).

[50] D. A. Stewart, arXiv:cond-mat/0606767 (unpublished).

[51] A. Khein, D. J. Singh, and C. J. Umrigar, Phys. Rev. B **51**, 4105 (1995).